Patterns of stress-strain behaviour for a clay till

Un schéma de contrainte-déformation d'une argile à blocaux

P. I. LEWIN, City University, London, UK (Formerly at the Building Research Station)
J. J. M. POWELL, Building Research Station, Watford, UK

SYNOPSIS

The paper analyses a set of consolidated undrained triaxial tests on a clay till. A normalising technique is suggested which adjusts the stress paths so that all the compression tests terminate at one single point, and all the extension tests at another single point, each according to the appropriate angle of shearing resistance ϕ'. From this one can draw an idealised undrained stress path behaviour pattern on which it is possible to superimpose axial strain contours.

INTRODUCTION

Although patterns of stress-strain behaviour have been established for several reconstituted soils (Rendulic 1937, Henkel 1958, Wroth and Loudon 1967) it is not easy to do the same for natural soils where the scatter of experimental results can swamp any underlying trends. The opportunity has been taken here to examine a set of undrained compression and extension triaxial tests in order to establish a pattern that gives a reasonable and useful description of both the stress paths and the strains measured during undrained loading from an all-round stress state.

The Building Research Establishment test-bed site at Cowden, North Humberside, U.K., is one that has been extensively investigated as part of a programme of work on the assessment of the engineering properties of glacial tills.

The soil profile (Powell, Marsland and Al-Khafaji, 1983) consisted of glacial clay tills, with occasional layers of sand, overlying chalk at about 60 metres depth. Natural water contents, after allowing for about 10% of the material which was retained in a BS 36 sieve, lay between 16 and 19%. The top 5 metres was mostly a firm to stiff dark brown chalky silty clay (PL 20%, LL40%) and below that there was a colour change to grey-brown (PL 18%, LL 36%). The clay size fraction was about 30%. All the clay contained inclusions of flints, chalk, sandstone, siltstone and coal particles.

The research programme included a comparison of loading tests on driven piles and bored piles. An extended range of triaxial tests was therefore required to cover both low consolidation pressures (to allow for swelling of the clay at a bored surface) and also high consolidation pressures (to allow for consolidation due to driving piles into the ground).

TEST PROGRAMME

The 100 mm diameter triaxial specimens were taken from the top 20 metres using thin walled sample tubes. Drainage during consolidation was allowed from both ends of the triaxial specimen using filter paper side drains. Greased rubber discs were used to relieve platen friction. Consolidation was carried out against a backpressure of two atmospheres. Where falls in pore pressure were expected, for example during the extension tests, the cell pressure at the end of consolidation was increased to ensure that the pore pressure would always remain suitably positive.

Isotropically consolidated triaxial tests were carried out on tube samples taken in July 1982. Three of these were tested in drained compression. One was tested in undrained compression. The remainder were tested in undrained tension. With the undrained tests it took about 2 hours to reach 0.5% strain - which was at about 25 to 50% of the deviator stress at failure. Also reported are twelve isotropically consolidated undrained compression tests carried out during 1977/78 on samples taken from close by on the same site and at comparable depths.

RESULTS

Stress Paths

Conventional assessment of triaxial test results is often concerned largely with the stress state at failure, which must be suitably defined. Taking failure as the situation at maximum deviator stress gave angles of shearing resistance ϕ' of 27^{o} for compression and -33^{o} for extension, both assuming a zero cohesion intercept c'. (The extension test failure line could have been assessed as ϕ' = -28.4^{o} and c' =-20 kPa but the effect over the working range of immediate undrained shear strengths, which lie between 80 kPa and 240 kPa, is minimal).

Much additional benefit can be derived from the collective behaviour of all the stress paths, compression and extension, as shown in Figure 1 where σ_v' (vertical effective stress) is plotted against $\sqrt{2}\,\sigma_H'$ (horizontal effective stress). This represents the paths in the axisymmetric $\sigma_x' = \sigma_y'$ plane of three dimensional principal stress space $\sigma_x'\ \sigma_y'\ \sigma_z'$.

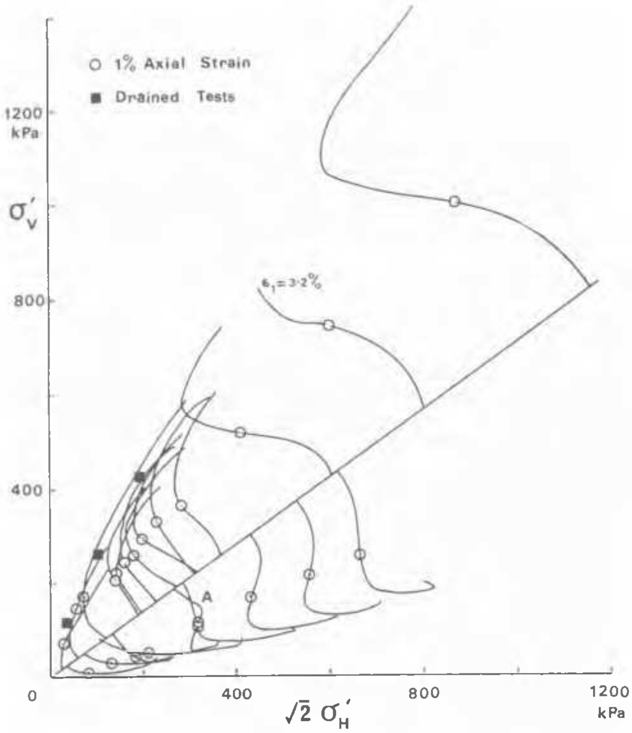

Fig.1 Undrained Stress Paths

Stress paths for conventional compression and extension tests starting from the same stress state may be visualised as the upper and lower 'ribs' of some three-dimensional surface sweeping round the stress space diagonal. If compression and extension tests are viewed as both contributing to a continuous surface, rather than just being unrelated opposites, then they serve to complement and corroborate each other.

An interesting feature of Figure 1 is that for those undrained tests starting from the same isotropic stress state, the stress paths in compression and extension finish up diametrically opposite each other with respect to the stress space diagonal - which indicates that they are then at the same mean effective stress p' - although they are clearly not equidistant from it so that strict rotational symmetry in $\sigma_x'\ \sigma_y'\ \sigma_z'$ space has not been achieved. This relationship is confirmed by Figure 2 which shows, for the condition at maximum deviator stress, the value of the mean effective stress p_f' plotted against the initial consolidation pressure p_o'. Although there is a suggestion that p_f' in compression is slightly greater than p_f' in extension, a single curve has been drawn through the results of both the compression and the extension tests. This is in accord with Randolph and Wroth (1981) who thought it reasonable to assume that the value of p_f', for a given water content of the soil, is independent of the mode of undrained shear. Over the range of values of p_o'=0 to 800 kPa, the relationship can be expressed approximately as $p_f' = 0.9\ p_o' + 100$.

It may be noted in passing that the value p_f'/p_o' serves the same purpose as the pore pressure parameter A_f (Skempton, 1954) since, taken together with ϕ', p_f'/p_o' determines both the pore pressure change and the deviator stress at failure; however, A_f has the disadvantage that, because of the way in which it is defined, the values in compression and extension are necessarily very different.

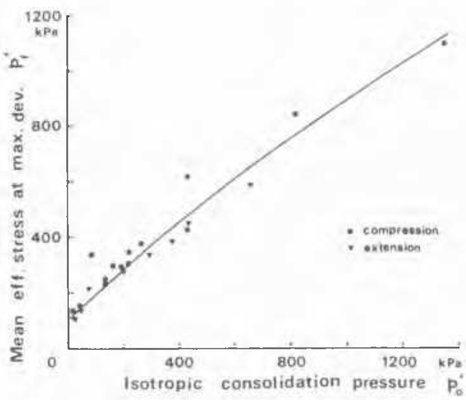

Fig.2 Relationship between mean effective stress at failure and the initial consolidation pressure

Although a basic behaviour pattern is already obvious from Figure 1, it is obscured by stress paths overlapping and by general experimental scatter. The results have therefore been replotted in Figure 4 although the stress path for one of the extension tests (see Fig. 1, marked A) has been omitted because its unusual shape possibly indicates some experimental irregularity. Use has been made of a normalising procedure in which the failure points of the stress paths are 'tethered' to the failure points that would arise from the mean ϕ' values of 27° (compression) and -33° (extension). This is feasible provided (a) ϕ' values are not dependant on consolidation pressures and (b) the c' intercepts are zero.

The method for adjusting and normalising the values of the principal effective stresses during each test is as follows. Adjusted values will be denoted by the additional suffix m.

(1) Recalculate the deviatoric stress q = $\sigma_V' - \sigma_H'$ as if failure had occurred at the mean value of ϕ'. Thus on the q p plot in Fig. 3, AB is the measured stress

path for a compression test. Using the mean value of ϕ' (ie 27^{o}) OF is drawn as obtained from the standard relationship $q_f/p_f = 6\sin\phi'/(3-\sin\phi')$. C, at the same value of p' as B, is the 'adjusted' point of failure. AC is drawn so that at any value of p' the measured value of q is increased in the ratio CD/BD to give q_m.

(2) Separate out the values of σ'_{Vm} and σ'_{Hm} by means of the standard relationship $\sigma'_V = p' + 2/3q$ and $\sigma'_H = p' - 1/3q$ but using q_m for q.

(3) Normalise σ'_{Vm} and σ'_{Hm} with respect to p'_f.

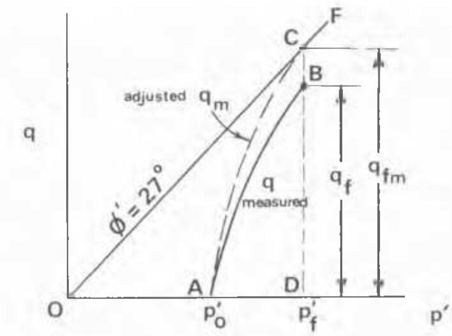

Fig.3 Method of adjusting stress path

The adjusted stress paths shown in Figure 4 represent a gathering together of the essential shapes of all the experimental stress paths. The pattern is seen to be substantially consistent and appears to be unaffected by either the stress history or the depth of the sample. An idealised pattern, which somewhat resembles an edge-on view of the shell of a Nautilus, can then be sketched as shown in

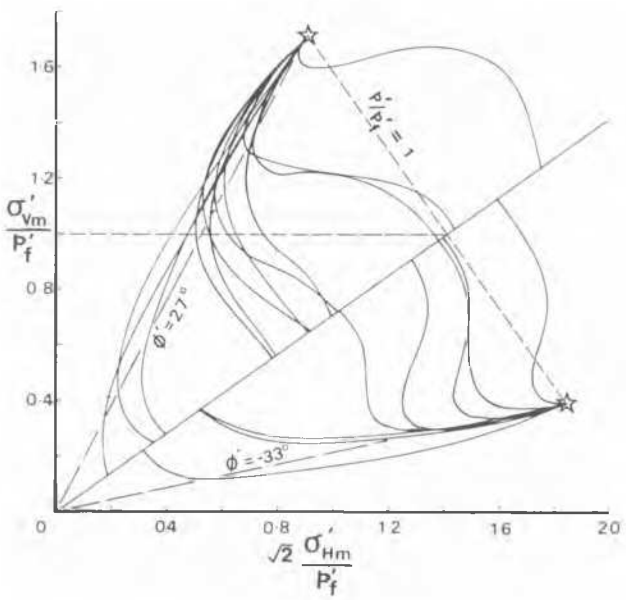

Fig.4 Adjusted normalised stress paths

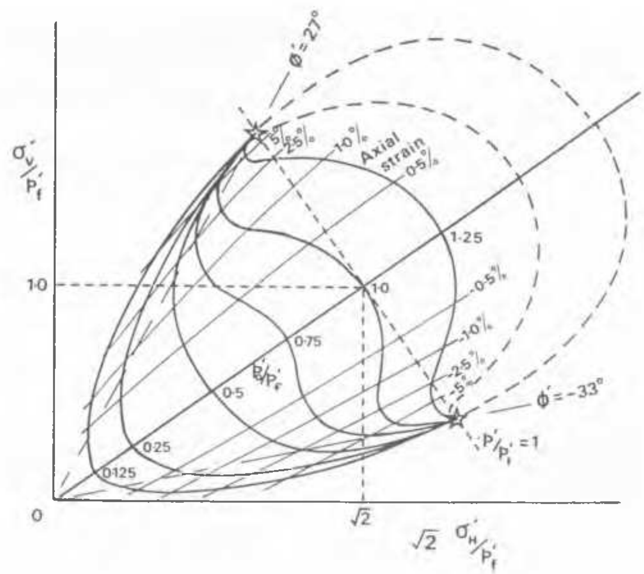

Fig.5 Idealised undrained pattern behaviour

Figure 5. Additional dotted lines have been drawn to suggest stress paths for samples consolidated to much higher consolidation pressures than were actually tested.

A highly significant feature in the shape of the stress paths shown in Figure 4 (and in Figure 5) is the fact that the paths bulge above the straight line joining the origin to the failure point. This emphasises the irrelevance of treating the maximum stress ratio as a criterion for failure since with the lower consolidation pressures this condition arises at strains as low as 1%. It also leads to the stress paths, as plotted collectively in Figure 1, tending to fall back and overlap each other thereby confusing the evidence for ascertaining a failure line. The fact of a stress path reaching, and even crossing, a failure line does not mean that the soil is failing or that it is in an unstable condition. It can be perfectly stable so long as there is no change in the drainage conditions.

Strains

The stress paths shown in Figure 1 have been marked at the point at which the strain was 1% and there is clear evidence of a behaviour which could enable one to draw a line connecting all these points on to a common strain contour. However if one tried to do the same for any higher value of strain there would be total confusion and the construction of a pattern of strain contours would be impossible.

To enable such strain contours to be drawn the following method has been adopted. From the individual test results, stress conditions have been ascertained for strains of 0.5, 1.0, 2.5 and 5.0%. These are shown in Figure 6 as the proportion of the deviator stress to failure for that test ie q/q_f plotted against p'_o/p'_f.

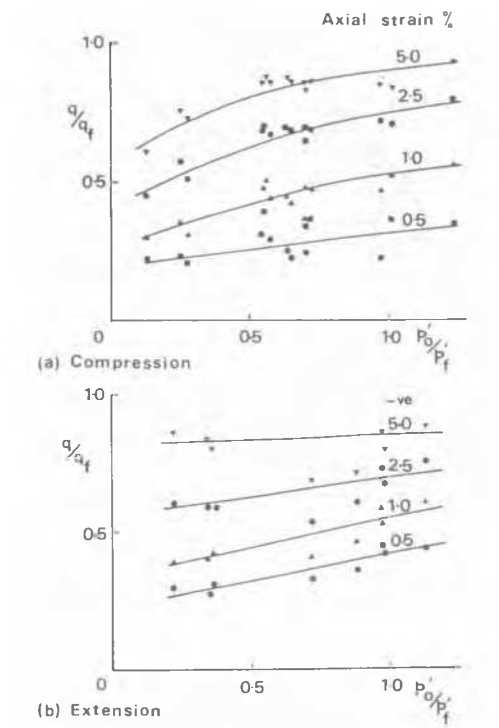

Fig.6 Strains at different levels of deviatoric stress

This has been done separately for compression and extension and mean lines have been drawn for each strain value. Using each strain line in turn, the deviator stress condition has been determined for p'_o/p'_f values 0.125, 0.25, 0.5, 0.75, 1.0 and 1.25. The appropriate points have been marked on the stress paths in Fig.5 and strain contours have been drawn accordingly.

CONCLUSION

Sophisticated analytical techniques that are currently available require parameters that give a much better description of the whole range of deformation than just ϕ', c' and A_f. It is essential therefore to gain some appreciation of the overall behaviour pattern. The difficulty is that experimental scatter, largely due to variability of the test material, can completely confuse the recognition of such a pattern. This paper suggests using a procedure for adjusting the test results in order to produce an idealised but realistic pattern (Figure 5) which, taken together with an expression relating p'_f to p'_o, is then a complete description of both the stress path and the strain behaviour for a set of consolidated undrained tests.

From such a pattern it should now be possible to derive a set of parameters which can then lend themselves to generalisation to deal with three-dimensional stress space and possibly be extended to deal with further complications such as the effect of stress history and anisotropy.

ACKNOWLEDGEMENT

The work described has been carried out as part of the research programme of the Building Research Establishment of the Department of the Environment and this paper is published by permission of the Director. Most of the compression tests were carried out by Mr. D. Williams and the extension tests were carried out by Mr. B.J. Eason and Mr. J. Dobbs.

REFERENCES

Henkel, D.J. (1960). The relationships between the effective stress and water content in saturated clays. Geotechnique 9, 3, 119-35.

Powell, J.J.M., Marsland, A. and Al-Khafaji, A.N. (1983). Pressuremeter testing of glacial clay tills. Int. Symp. on In Situ Testing, Paris, 2, 373-8.

Randolph, M.F. and Wroth, C.P. (1981). Application of the failure state in undrained simple shear to the shaft capacity of driven piles. Geotechnique 31, 1, 143-57.

Rendulic, L. (1936). Relation between void ratio and effective principal stresses for a remoulded silty clay. 1st ICSMFE, Harvard, 3, 48-51.

Skempton, A.W. (1954). The pore pressure coefficients A and B. Geotechnique 4, 143-147.

Wroth, C.P. and Loudon, P.A. (1967). The correlation of strains within a family of triaxial tests on overconsolidated samples of kaolin. Proc. Geot. Conf., Oslo 1, 159-63.